NANO LETTERS

Letter

pubs.acs.org/NanoLett

Ultralow Thermal Conductivity in Organoclay Nanolaminates Synthesized via Simple Self-Assembly

Mark D. Losego,[†] Ian P. Blitz,[‡] Richard A. Vaia,[§] David G. Cahill,*[,†] and Paul V. Braun*[,†]

[†]Department of Materials Science and Engineering, University of Illinois, Urbana Illinois 61801, United States

[‡]Department of Chemistry, University of Illinois, Urbana Illinois 61801, United States

[§]Materials and Manufacturing Directorate, Air Force Research Laboratory, Wright-Patterson AFB, Ohio 45433, United States

Supporting Information

ABSTRACT: Because interfaces impede phonon transport of thermal energy, nanostructuring can transform fully dense solids into ultralow thermal conductivity materials. Here we report a simple self-assembly approach to synthesizing organoclay nanolaminates with cross-planar thermal conductivities below 0.10 W m^{-1} K^{-1}—a 5-fold decrease compared to unmodified clay. These organoclays are produced via alkylammonium cation exchange with colloidally dispersed montmorillonite clay sheets followed by solvent casting. Time-domain thermoreflectance (TDTR) is used to evaluate the thermal conductivity of the organoclay nanolaminates. Variations in both organic layer thickness and cation chemistry are investigated. At these interface densities (1.0−1.5 interfaces/nm), we demonstrate that thermal conductivity is relatively independent of nanolaminate spacing. A simple series resistance model describes the behavior and gives an interfacial thermal conductance value of ≈150 MW m^{-2} K^{-1} for the organic/clay interface, consistent with similar organic−inorganic interfaces. The wide range of compositional substitutions and structural variations possible in these materials, make organoclays a versatile new platform for investigating the underlying physics of nanolaminate structures.

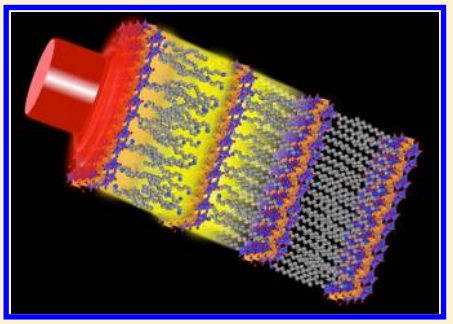

KEYWORDS: *Thermal conductivity, organoclay, self-assembly, nanolaminate, interfacial thermal conductance*

For phonon-mediated heat conduction, a material is generally thought to reach its lowest thermal conductivity (Λ) when amorphous, forcing heat to travel via a random walk of atomic vibrations.[1] However, this "amorphous limit" can be surpassed when nanoscale features are introduced.[2−5] An important class of ultralow thermal conductivity materials (Λ < 0.1 W m^{-1} K^{-1}) is those formed from nanoscale multilayers, commonly referred to as "nanolaminates". These nanolaminates can be treated as a series of thermal resistors. Because interfaces scatter phonons, they provide additional thermal resistance to the system. Interface densities in nanolaminates can be sufficiently high to reduce the thermal conductivity to below the amorphous limit.[2,6−8] The thermal conductivity of nanolaminates can be further reduced by decreasing the interface's thermal conductance (G). Decreases in G are possible by selecting materials with disparate acoustic properties[6,9] or reducing the interfacial bonding stiffness.[10]

Molecular beam deposited WSe_2 films having a turbostratic, layered structure exhibit the lowest known thermal conductivity for a fully dense solid ($\Lambda \approx 0.06$ W m^{-1} K^{-1} at room temperature).[11] This atomic-scale laminate material consists of WSe_2 sheets (0.66 nm thick) with strong intraplanar covalent bonding and weak interplanar van der Waals bonding. Theoretical investigations suggest that the low interfacial bond stiffness combines with rotational disorder in WSe_2 sheet stacking to impede coherent cross-planar vibrations by both introducing a low interfacial thermal conductance and effectively focusing phonons within the covalently bonded sheets.[12] However, verification of these theories requires expanding experimental investigations to a larger materials set where these parameters can be systematically adjusted. Moreover, if this combination of nanoscale structural features could be incorporated into an electrically conductive material, these systems would present opportunities for a new class of thermoelectric materials.

Because clays adopt a naturally self-assembled nanolaminate structure consisting of aluminosilicate sheets separated by intercalated cationic species with ≈1 nm spacing, these materials are obvious candidates for achieving ultralow thermal conductivities. The structure of clays can also be adjusted using well-known methods of cation exchange.[13] By exchanging with cationic organic molecules, "organoclays" can be synthesized. Here we examine the thermal transport properties of organically modified montmorillonite clays that have been spun-cast into nanolaminate thin film structures. Unlike WSe_2 films, which require synthetically complicated molecular beam deposition tools, clay-based nanolaminate films can be deposited using simple, solution-phase methods, and through cation exchange, structural features like laminate spacing and

Received: February 26, 2013
Revised: April 12, 2013

   dx.doi.org/10.1021/nl4007326 | *Nano Lett.* XXXX, XXX, XXX−XXX

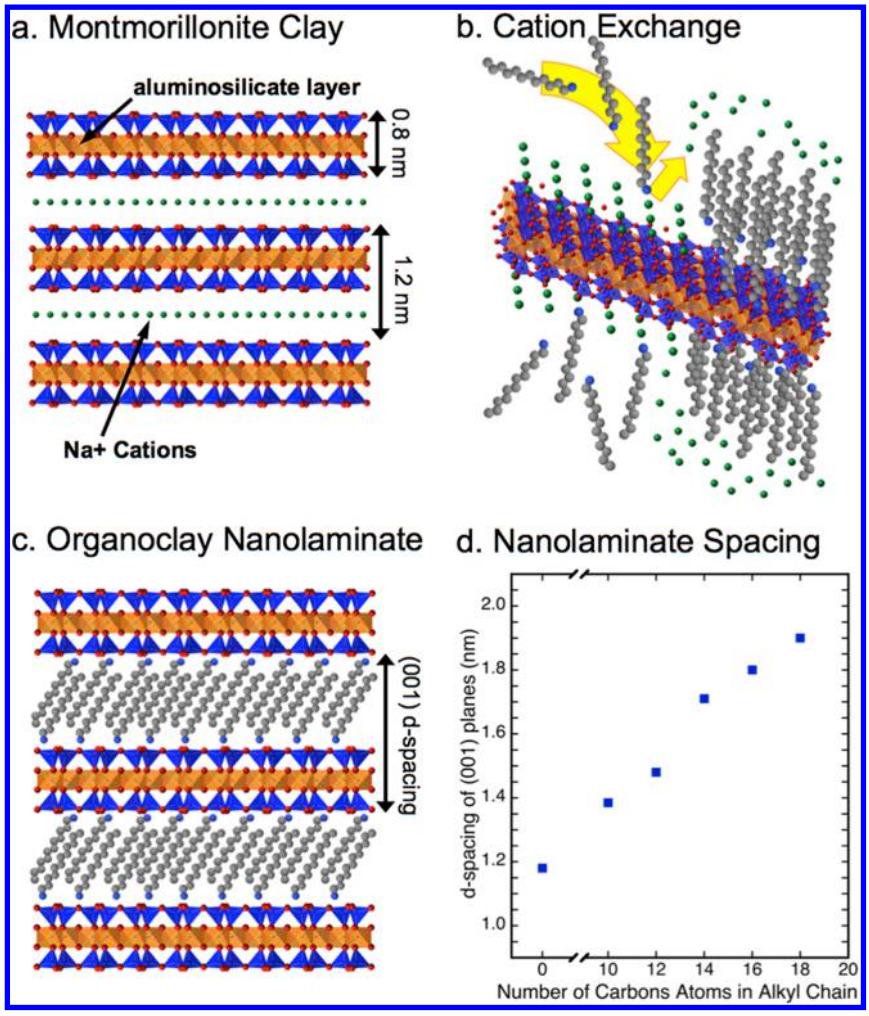

Figure 1. (a) Crystal structure of Na-montmorillonite clay. Intercalated sodium ions are green, oxygen atoms are red, corner-shared silica tetrahedrons are blue, and edge-shared alumina octahedrons are orange. (b) Scheme illustrating alkylammonium cation exchange. (c) Structure of idealized organoclay nanolaminates. Carbon atoms are gray, and nitrogen is blue. (d) *d*-spacing of (001) planes in organoclay nanolaminates determined from the position of the 001 reflection in $\theta-2\theta$ X-ray diffraction scans.

interfacial bonding stiffness can be adjusted. Cross-planar thermal transport of intercalated clays also has implications for flame retardance in clay-loaded polymers where low thermal conductivity of charred clay is thought to reduce polymer flammability.[14] Here we demonstrate that ultralow thermal conductivities ($\approx$ 0.08 W m^{-1} K^{-1}) can be reached in montmorillonite-based organoclay nanolaminates modified with alkylammonium cations.

As pictured in Figure 1a, montmorillonite consists of crystalline aluminosilicate sheets having a net negative charge that is balanced by intercalated sodium ions (Na^+). By sonicating a montmorillonite dispersion, this clay is exfoliated into $\approx$0.8 nm thick crystalline sheets with large aspect ratios (in excess of 100:1).[15] Within solution, the compensating Na^+ cations can be exchanged with various positively charged species including organic cations. For these experiments, Na^+ is exchanged with primary alkylammonium cations of varying alkyl chain lengths and headgroup chemistries. The terminal cation of the alkylammonium molecule associates with the surface of the montmorillonite sheets (Figure 1b). After workup, these organically modified clay sheets can be redispersed in solution and spun-cast onto a substrate. Upon spin-casting and solvent evaporation, the clay reassembles to form a nanolaminate (Figure 1c) of alternating high (aluminosilicate layer) and low (organic layer) elastic modulus materials (see Supporting Information for detailed experimental procedures). By adjusting the alkyl chain length of the ammonium cation, the interplanar spacing can be tuned (Figure 1d). Differential scanning calorimetry (DSC) measurements of the organoclays show a weak glass transition at approximately 85 °C (Supporting Information, Figure S3), suggesting that the organic component of the structure is glassy at room temperature.

Cross-planar thermal conductivity is measured by time-domain thermoreflectance (TDTR), an optical measurement technique using an ultrafast pump−probe arrangement.[2] To make the measurement, a metal film is deposited on the clay surface to act as both a light-to-heat transducer and an optical thermometer. Measurements are made with a Ti:sapphire mode-locked laser that is split into two pulsed beams. The metal layer absorbs the pump pulses, generating a temperature rise. The probe pulses monitor surface temperature via thermoreflectance as a function of time after the initial heating pulse. Thermal conductivity is then extracted by fitting the TDTR data to a thermal diffusion model.[16]

dx.doi.org/10.1021/nl4007326 | *Nano Lett.* XXXX, XXX, XXX−XXX

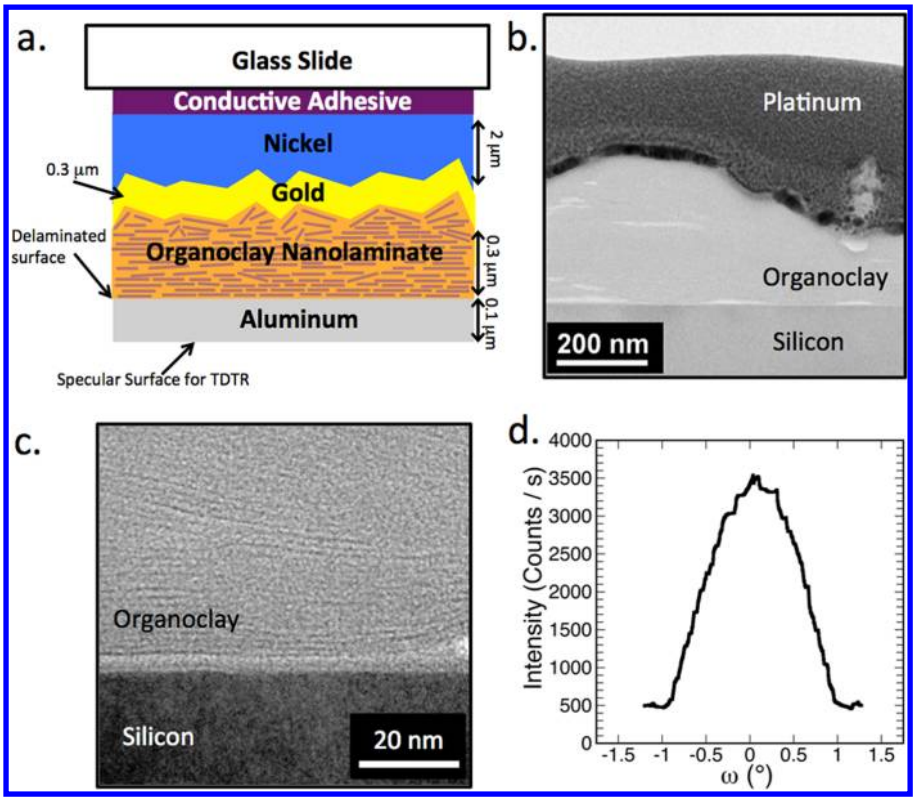

Figure 2. (a) Schematic of the sample geometry used for TDTR measurements. Low (b) and high (c) magnification cross-section TEM images of spun-cast organoclays on silicon. Platinum was added to aid in TEM sample preparation. (d) Representative X-ray diffraction rocking curve collected for the 001 reflection of an organoclay nanolaminate film spun-cast on silicon.

A specular reflective surface is important for proper TDTR signal collection. The top surface of spun-cast clay films are too rough for TDTR measurements (see Figure S2 of the SI). To achieve sufficient specularity, the films are delaminated from their silicon substrates revealing a smooth surface appropriate for TDTR. Prior to delamination, a heat sink is added to the rough top surface, consisting of a sputter deposited Cr/Au layer, a ≈ 2 μm electroplated nickel layer, and a thermally conductive adhesive (Dow Corning 3-1818) as pictured in Figure 2a and detailed in the Supporting Information, including Figure S1. Once delaminated, aluminum is sputtered on the smooth clay surface to act as the thermal transducer and temperature monitor.

Inversion of the film also exposes an organoclay nanolaminate structure with parallel stacking of the aluminosilicate sheets (Figure 2). The X-ray diffraction rocking curves for the 001 reflection show a narrow distribution of intensity in-plane with the surface. A representative rocking curve measurement is shown in Figure 2d (additional scans are shown in Figure S6). These rocking curves suggest that the (001) aluminosilicate sheets are aligned parallel with the surface. Based on the rocking curves' full-width-half-maxima, we conclude that a majority of the aluminosilicate sheets are misaligned by <1.5°. Cross-sectional transmission electron microscopy (TEM) images (Figure 2b,c) corroborate this conclusion. Prior to inversion, TEM images reveal that aluminosilicate sheets near the substrate show <3° misalignment with the silicon surface, although disorder does increase farther from this interface.

Thermal modeling (see Figure S7 in SI) shows that our TDTR measurements are sensitive to the thermal properties of the organoclay nanolaminate structure within ≈50 nm of the surface. Therefore, misalignment of the layered structure at distances farther than ≈50 nm from the surface will not affect the measurement. TEM imaging suggests that the misalignment of the layers is <3° at distances up to 25 nm from the surface. Assuming an anisotropy in Λ of 10:1, we estimate that clay layers tilted at 3° would exhibit 3% higher thermal conductivities than the true cross-planar value. At depths beyond 25 nm, we estimate that about 20−30% of the clay sheets exhibit up to 20° misalignment which would increase thermal conductivity by 120%. This corresponds to $\Lambda \approx 0.2$ W m^{-1} K^{-1}. Making the extreme assumption that the entire organoclay layer beyond 25 nm in depth has a thermal conductivity of 0.2 W m^{-1} K^{-1}, we find that our error in fitting to the true cross-planar thermal conductivity is only ±0.01 W m^{-1} K^{-1}. This analysis suggests that our TDTR measurements provide a good approximation for the cross-planar thermal conductivity of the organoclay nanolaminate, within about 11% error.

Figure 1d demonstrates the use of cation exchange to vary the lattice parameter and interface density of the organoclay nanolaminate. By exchanging the clay's cations with alkylammonium molecules of 10−18 carbon atoms in length, the (001) lattice parameter systematically increases from ≈1.2 nm to ≈1.9 nm. Estimating an aluminosilicate layer thickness of ≈0.8 nm implies that the organic component varies in thickness from ≈0.4 nm to ≈1.1 nm and constitutes between 33% and 58% of the structure by volume. The short organic spacing suggests that the alkyl chains are likely intercalated and not fully extended perpendicular to the clay sheets. Accounting for the two organic/inorganic interfaces per unit cell length, interface densities in these organoclay nanolaminates range from about 1 to 1.5 interfaces/nm. In comparison, the unmodified clay has 1 interface per unit cell length and 0.85 interfaces/nm.

dx.doi.org/10.1021/nl4007326 | Nano Lett. XXXX, XXX, XXX−XXX

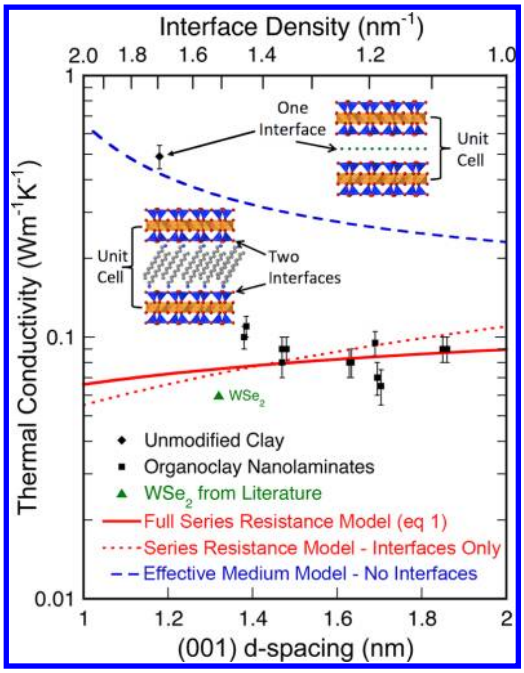

Figure 3. Measured values for the cross-planar thermal conductivity of unmodified Na-montmorillonite clay and organoclay nanolaminates prepared from varying alkylammonium chain lengths. The blue dashed line is an "effective medium" model that excludes interfacial conductance, the red dotted line assumes only interfacial conductance with G = 110 MW m^{-2} K^{-1}, and the red solid line is a series resistance model that includes organic layer conductance, aluminosilicate conductance, and interfacial conductance with G = 150 ± 10 MW m^{-2} K^{-1}. For reference, the thermal conductivity of WSe_2 is plotted at its equivalent interface density. Inset images illustrate our assumptions of 1 interface per unit cell for the unmodified clay and 2 interfaces per unit cell for the organoclays. The unmodified clay is plotted using its measured d-spacing but has an assumed interface density of 0.85 interfaces/nm.

Figure 3 plots the thermal conductivity of unmodified montmorillonite and each organoclay nanolaminate as a function of alkyl ammonium chain length. TDTR measurements reveal that all investigated organoclay nanolaminates have a thermal conductivity of ≈0.09 W m^{-1} K^{-1}. This value is lower than typical amorphous organics (liquid dodecane = 0.14 W m^{-1} K^{-1}, amorphous polymethyl methacrylate = 0.20 W m^{-1} K^{-1}) and 5 times lower than the thermal conductivity we have measured for the unmodified clay (0.48 W m^{-1} K^{-1}). It is also one of the lowest thermal conductivities ever reported for a fully dense solid.

We construct a simple series resistance model to better understand the influence of interfacial thermal conductance in these nanolaminates:

$$\frac{d}{\Lambda_{\text{effective}}} = \sum_{\text{unitcell}} \frac{t_i}{\Lambda_i} + \sum_{\text{unitcell}} \frac{1}{G_i} \quad (1)$$

where $\Lambda_{\text{effective}}$ is the thermal conductivity we measure, d is the unit cell spacing in the heat flow direction, t_i is the layer thickness (organic or aluminosilicate), Λ_i is the layer thermal conductivity, and G_i is the interfacial thermal conductance. For our modeling we estimate the organic layer to have thermal properties akin to liquid dodecane (0.14 W m^{-1} K^{-1}) and the aluminosilicate layer to have a thermal conductivity of 2 W m^{-1} K^{-1}, similar to the amorphous limit of Al_2O_3. For the organoclays, we assume G_i is the same for all of the organic/inorganic interfaces regardless of chain length or heat flow direction, and we model the system as two interfaces per unit cell as depicted in the inset of Figure 3. The blue dashed line in Figure 3 assumes no interface effects (i.e., ignores the second term in eq 1). Consistent with previous findings,[6,7] this effective medium model overestimates the thermal conductivity of the experimental observations (similarity to the unmodified clay is coincidental). By ignoring the first term in eq 1 and only considering interfacial effects (red dotted line), we can adequately fit the data using G = 110 ± 10 MW m^{-2} K^{-1}. However, the measured data appears to have less dependence on interplanar spacing than this model predicts. By including all terms in eq 1 (red solid line), we find a model that better fits this flat response over the probed thickness range. This model indicates an interfacial thermal conductance of 150 ± 10 MW m^{-2} K^{-1} (based on a ± 0.2 nm uncertainty in determining the van der Waals atom-to-atom distance of the clay sheet thickness). This value is consistent with, but on the higher end of, comparable organic/inorganic interfaces.[8−10,17] Discrepancy between the data and this model at the shortest chain lengths may indicate a change in interfacial conductance caused by differences in molecular ordering.

Treating the intercalated sodium cations as a single interface, the unmodified clay has a significantly lower interface density (0.85 interfaces/nm) than the organoclay nanolaminates (1.0−1.5 interfaces/nm). However, this does not fully explain its higher thermal conductivity. The unmodified clay must also have a higher interfacial thermal conductance, which we estimate to be 400 ± 20 W m^{-2} K^{-1}. The WSe_2 system has an interface density (1.52 interfaces/nm) similar to the organoclay nanolaminates. Based on the published data, we estimate that the organoclay nanolaminates have a 1.7× higher interfacial thermal conductance than the WSe_2 system ($G_{WSe_2} \approx \Lambda/t$ = 0.06 W m^{-1} K^{-1}/0.66 nm = 90 MW m^{-2} K^{-1}). These differences cannot be fully explained by any measurement errors associated with clay sheet misalignment. We hypothesize that differences in the elastic moduli of the layers are affecting interfacial thermal transport and dictating the thermal conductivity of the nanolaminates.

We have also prepared organoclay nanolaminates with identical chain lengths (dodecyl) but varying ammonium functionalizations in an attempt to modify interfacial bonding stiffness. Measured thermal conductivities for these organoclays are reported in Figure 4. Recent simulations, theory, and experiments[10,18,19] have demonstrated the ability to use interfacial bond stiffness to vary G. Here, this modification of G would manifest as a change in the measured thermal conductivity of the nanolaminate. Within our measurement error, most of the chemistries investigated here have thermal conductivities between 0.8 and 0.9 W m^{-1} K^{-1}, which corresponds to G = 140−180 MW m^{-2} K^{-1}. However, the organoclay intercalated with trimethyl terminated dodecylammonium cations exhibits a measurable increase in thermal conductivity (0.11 W m^{-1} K^{-1}). This corresponds to G increasing to 240 MW m^{-2} K^{-1}.

In summary, ultralow thermal conductivity is possible in nanolaminate systems synthesized via simple self-assembly. Low temperature synthesis of organoclay nanolaminates avoids interfacial intermixing and promotes abrupt interfaces. The average thermal conductivity for these nanolaminates (0.09 W m^{-1} K^{-1}) approaches that of the lowest ever reported in a dense solid, 0.06 W m^{-1} K^{-1} for WSe_2 films produced by more

dx.doi.org/10.1021/nl4007326 | Nano Lett. XXXX, XXX, XXX−XXX

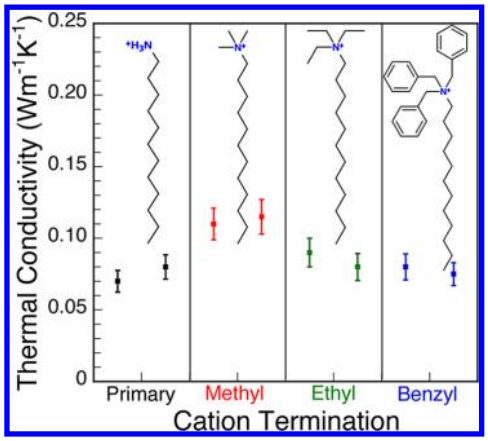

Figure 4. Thermal conductivities for organoclay nanolaminates modified with alkyl ammonium cations of similar alkyl chain length (dodecyl) but varying ammonium cation chemistries.

complex molecular beam evaporation techniques. Simple series resistance modeling suggests that the interface densities achieved in these organoclays (1−1.5 interfaces/nm) are sufficient to attain these ultralow thermal conductivities. Using this model, we determine an average interfacial thermal conductance of 150 MW m^{-2} K^{-1} for the organic/clay sheet interfaces. Because considerably lower interfacial conductances with molecular layers are possible (<50 MW m^{-2} K^{-1}),[10] opportunity exists for designing nanolaminate materials with even lower thermal conductivities. Thus, organoclays are poised to become a versatile experimental platform for exploring and validating the thermal physics of nanolaminate materials.

■ ASSOCIATED CONTENT

Ⓢ Supporting Information

Description of organoclay synthesis and preparation for TDTR measurements, TDTR analysis, and additional structural characterization. This material is available free of charge via the Internet at http://pubs.acs.org.

■ AUTHOR INFORMATION

Corresponding Author

*E-mail: d-cahill@illinois.edu, pbraun@illinois.edu.

Notes

The authors declare no competing financial interest.

■ ACKNOWLEDGMENTS

We thank Professor Jeff Moore for use of his DSC system and Dr. Dong-Wook Oh for assistance with the RBS measurements. This work is supported by the Air Force Office of Scientific Research (AFOSR) MURI FA9550-08-1-0407. Fabrication and characterization were carried out in part in the Frederick Seitz Materials Research Laboratory at the University of Illinois Urbana−Champaign, which is partially supported by the U.S. Department of Energy under grants DE-FG02-07ER46453 and DE-FG02-07ER46471.

■ REFERENCES

(1) Cahill, D. G.; Watson, S. K.; Pohl, R. O. *Phys. Rev. B* **1992**, *46* (10), 6131−6140.
(2) Cahill, D. G.; Ford, W. K.; Goodson, K. E.; Mahan, G. D.; Majumdar, A.; Maris, H. J.; Merlin, R.; Phillpot, S. R. *J. Appl. Phys.* **2003**, *93* (2), 793−818.
(3) Kim, W.; Zide, J.; Gossard, A.; Klenov, D.; Stemmer, S.; Shakouri, A.; Majumdar, A. *Phys. Rev. Lett.* **2006**, *96* (4), 045901.
(4) Lee, S. M.; Cahill, D. G.; Venkatasubramanian, R. *Appl. Phys. Lett.* **1997**, *70* (22), 2957−2959.
(5) Lee, M. L.; Venkatasubramanian, R. *Appl. Phys. Lett.* **2008**, *92* (5), 053112.
(6) Costescu, R. M.; Cahill, D. G.; Fabreguette, F. H.; Sechrist, Z. A.; George, S. M. *Science* **2004**, *303* (5660), 989−990.
(7) Alvarez-Quintana, J.; Peralba-Garcia, L.; Labar, J. L.; Rodriguez-Viejo, J. *J. Heat Transfer-Trans. ASME* **2010**, *132* (3), 032402.
(8) Jin, Y.; Yadav, A.; Sun, K.; Sun, H.; Pipe, K. P.; Shtein, M. *Appl. Phys. Lett.* **2011**, *98* (9), 093305.
(9) Ong, W.-L.; Rupich, S. M.; Talapin, D. V.; McGaughey, A. J. H.; Malen, J. A. *Nat. Mater.* **2013**, DOI: 10.1038/nmat3596.
(10) Losego, M. D.; Grady, M. E.; Sottos, N. R.; Cahill, D. G.; Braun, P. V. *Nat. Mater.* **2012**, *11* (6), 502−506.
(11) Chiritescu, C.; Cahill, D. G.; Nguyen, N.; Johnson, D.; Bodapati, A.; Keblinski, P.; Zschack, P. *Science* **2007**, *315* (5810), 351−353.
(12) Wei, Z.; Chen, Y.; Dames, C. *Appl. Phys. Lett.* **2013**, *102* (1), 011901.
(13) Heinz, H.; Vaia, R. A.; Krishnamoorti, R.; Farmer, B. L. *Chem. Mater.* **2007**, *19* (1), 59−68.
(14) Gilman, J. W.; Jackson, C. L.; Morgan, A. B.; Harris, R.; Manias, E.; Giannelis, E. P.; Wuthenow, M.; Hilton, D.; Phillips, S. H. *Chem. Mater.* **2000**, *12* (7), 1866−1873.
(15) Cao, T.; Fasulo, P. D.; Rodgers, W. R. *Appl. Clay Sci.* **2010**, *49* (1−2), 21−28.
(16) Cahill, D. G. *Rev. Sci. Instrum.* **2004**, *75* (12), 5119−5122.
(17) Losego, M. D.; Moh, L.; Arpin, K. A.; Cahill, D. G.; Braun, P. V. *Appl. Phys. Lett.* **2010**, *97* (1), 011908.
(18) Prasher, R. *Appl. Phys. Lett.* **2009**, *94* (4), 041905.
(19) Hu, M.; Keblinski, P.; Schelling, P. K. *Phys. Rev. B* **2009**, *79* (10), 104305.

dx.doi.org/10.1021/nl4007326 | *Nano Lett.* XXXX, XXX, XXX−XXX